

# Synthesis, Characterization, and Fluorescence Quenching of Novel Cationic Phenyl-Substituted Poly(*p*-phenylenevinylene)s

Qu-Li Fan and Su Lu

*Institute of Materials Research and Engineering, National University of Singapore, 3 Research Link, Singapore 117602, Republic of Singapore*

Yee-Hing Lai

*Department of Chemistry, National University of Singapore, 10 Kent Ridge Crescent, Singapore 119260, Republic of Singapore*

Xiao-Yuan Hou and Wei Huang\*

*Institute of Advanced Materials, Fudan University, 220 Handan Road, Shanghai 200433, The People's Republic of China*

*Received February 5, 2003; Revised Manuscript Received July 16, 2003*

**ABSTRACT:** Three new phenyl-substituted poly(*p*-phenylenevinylene) (Ph-PPV) derivatives with amino-functionalized groups were synthesized through either Gilch reaction for poly{2,5-bis[4'-2-(*N,N*-diethylamino)ethoxyphenyl]-1,4-phenylenevinylene} (**P1**) or Wittig reaction for poly{2,5-bis(4'-decyloxyphenyl)-1,4-phenylenevinylene-*alt*-2,5-bis[4'-2-(*N,N*-diethylamino)ethoxyphenyl]-1,4-phenylenevinylene} (**P2**) and poly(2,5-bis[4'-2-[2-(2-methoxyethoxy)ethoxy]ethoxyphenyl]-1,4-phenylenevinylene-*alt*-2,5-bis[4'-2-(*N,N*-diethylamino)ethoxyphenyl]-1,4-phenylenevinylene) (**P3**). Green light-emitting cationic polymers, poly{2,5-bis(4'-decyloxyphenyl)-1,4-phenylenevinylene-*alt*-2,5-bis[4'-2-(*N,N,N*-triethylammonium)ethoxyphenyl]-1,4-phenylenevinylene} dibromide (**P2'**) and poly(2,5-bis[4'-2-[2-(2-methoxyethoxy)ethoxy]ethoxyphenyl]-1,4-phenylenevinylene-*alt*-2,5-bis[4'-2-(*N,N,N*-triethylammonium)ethoxyphenyl]-1,4-phenylenevinylene) dibromide (**P3'**), were prepared from the neutral polymers **P2** and **P3**, respectively. Water solubility was achieved on **P3'** through increase of the hydrophilicity of the side chains. The acid-assistant reversible solubility of **P1** makes it promising in preparing light-emitting multilayer devices. On the basis of FT-IR and <sup>1</sup>H NMR spectra, it was found that **P1** is primarily of *trans*-vinyl while **P2** and **P3** are of 80% and 81% *cis*-vinyl, respectively, which depends on the polymerization method employed. The bulky phenyl substituents successfully impeded the interchain interaction which led to quantum efficiency as films comparable to that of solutions. Quaternization also resulted in more twisted conformation of the polymer main chain which was supported by both blue-shifted absorption and reduced quantum efficiency of **P2'** and **P3'** in solutions and as films than that of the neutral polymers. The fluorescence of **P3'** was efficiently quenched by an anionic quencher Fe(CN)<sub>6</sub><sup>4-</sup>, *K*<sub>sv</sub> of which is  $3.3 \times 10^6 \text{ M}^{-1}$ . However, a modified Stern–Volmer plot showed that 9% of the fluorophores could not be accessible to the quencher, which may result from the twisted conformation or intermolecular aggregation.

## Introduction

Water-soluble conjugated polymers (WSCPs) have attracted increasing attention recently due to their versatile applications in optoelectronic<sup>1–3</sup> and biological research.<sup>4</sup> To endow conjugated polymers with water solubility, hydrophilic substituents such as quaternized ammonium, carboxylate, or sulfonate must exist on the polymer backbone which produce conjugated polyelectrolytes. The optical and electronic properties of WSCPs can be easily tuned by designing the conjugated structure of the polymer main chain. Furthermore, the ionic functionality was also found to be useful in the construction of interesting supramolecular structures with electronic activity.<sup>5–8</sup>

Envisioned applications of WSCPs include optoelectronic devices fabricated through layer-by-layer self-assembly,<sup>9</sup> ink-jet printing,<sup>10</sup> or screen printing techniques.<sup>11</sup> These new film deposition techniques may be promising in producing large area multilayer assemblies in a low-cost way. For example, Yang et al. developed

blue and orange-red dual-color polymeric light-emitting pixels via the hybrid ink-jet printing method (HIJP).<sup>12</sup> Rubner et al. reported sequentially adsorbed multilayer devices through layer-by-layer processing technique based on blue-light emitting polycation- and polyanion-type conjugated polymers.<sup>2</sup> The same strategy was also employed to study the Förster energy transfer between conjugated polymers of different band gaps.<sup>13</sup> Another reason for the current growing interest in these water-based techniques is to avoid the unfavorable interdiffusion or erosion between neighboring layers encountered in the organic solvent-based fabrication processes.<sup>14</sup> It is important to note, however, that polymers with red, green, and blue emission are required to obtain full-color displays. Water-soluble poly(*p*-phenylene) (PPP)<sup>15–17</sup> and poly(*p*-phenylenevinylene) (PPV),<sup>18,19</sup> which are blue and red light-emitting materials, respectively, have been investigated, while the preparation of water-soluble polymers with green emission is still a challenge.

Recently, WSCPs have also been found potential applications as high-sensitive biosensors which exhibit rapid and collective response to relatively small perturbations in local environment.<sup>20</sup> It has been shown that a low concentration of quencher is sufficient to extin-

\* To whom correspondence should be addressed: Tel +86 (21) 5566 4188, Fax +86 (21) 6565 5123; e-mail wei-huang@fudan.edu.cn/chewh@nus.edu.sg.

guish the fluorescence from the conjugated segments through electron transfer or energy transfer due to facile energy migration along the conjugated backbone and relatively strong binding of the quencher with WSCPs. Although such an amplified quenching has been achieved by using a few WSCPs including water-soluble PPV<sup>21</sup> and PPP<sup>22</sup> systems, the influence of the physical and chemical properties of these WSCPs such as chemical structures, fluorescent quantum efficiencies, and emission wavelength on the quenching sensitivity is still a major concern. Therefore, it is crucial to develop novel WSCPs to evaluate a variety of polymer compositions for obtaining optimized sensory materials.

In this paper, we report our successful effort in synthesizing a new series of water-soluble green light-emitting polymers, which should shed some light on problems raised above. Phenyl-substituted PPV derivatives are desired as they have proven to exhibit highly efficient green fluorescence and enhanced photostability due to the steric hindrance of the bulky phenyl groups which minimize the interchain interactions.<sup>23–25</sup> We are also very interested in cationic WSCPs because such systems are less studied<sup>17b,21g,26</sup> than the anionic counterparts in optoelectronic devices and sensors. Therefore, novel phenyl-substituted PPVs with tertiary amine functionality were prepared by using either Gilch or Wittig reactions. Water solubility was rendered to these materials via postquaternization on the neutral precursors with bromoethane. Besides, the water solubility was further studied through adjusting the hydrophilicity of the substituents. The optical and thermal properties of these novel water-soluble phenyl-substituted PPVs were characterized. The quenching behavior with an inorganic compound was also investigated. Preliminary results indicate that these materials offer promising opportunities in optoelectronic and sensory applications.

## Experimental Section

**General Methods.** The NMR spectra were collected on a Bruker Advance 400 spectrometer with tetramethylsilane as the internal standard. FT-IR spectra were recorded on a Bio-Rad FTS 165 spectrometer by dispersing samples in KBr. Mass spectra (MS) were obtained using a micromass VG 7035E mass spectrometer at an ionizing voltage of 70 eV. UV-vis spectra were recorded on a Shimadzu 3101 PC spectrometer. The concentrations of copolymer solutions were adjusted to about 0.01 mg/mL or less. Fluorescence measurement was carried out on a Perkin-Elmer LS 50B photoluminescence spectrometer with a xenon lamp as a light source. TGA measurements were performed on a TA Instruments Hi-Res TGA 2950 thermogravimetric analyzer at a heating rate of 10 °C/min under N<sub>2</sub>. Elemental microanalyses were carried out by the Microanalysis Laboratory of the National University of Singapore. Gel permeation chromatography (GPC) analysis was conducted with a Waters 2690 separation module equipped with a Waters 2410 differential refractometer HPLC system and three 5  $\mu$ m Waters Styragel columns (pore size: 10<sup>3</sup>, 10<sup>4</sup>, and 10<sup>5</sup> Å) in series, using polystyrenes as the standard and tetrahydrofuran (THF) as the eluant at a flow rate of 1.0 mL/min and 35 °C.

The quenching behavior was studied by comparing the fluorescence intensities of polymer aqueous solutions in the presence of quenchers with different concentrations. The Milli-Q water used in preparing the aqueous solutions of those polymers and quenchers was purged with nitrogen for 4 h before using.

**Materials.** All chemical reagents used were purchased from Aldrich Chemical Co. THF was purified by distillation from sodium in the presence of benzophenone. Other organic solvents were used without any further purification. Thionyl chloride was distilled prior to use.

**Synthesis. a. Procedure for the Preparation of P1 via Gilch Reaction.** A 0.315 g (0.5 mmol) sample of monomer **1** was added into 30 mL of anhydrous THF in a 50 mL round-bottom flask. To this stirred solution was added dropwise 4 mL of 1.0 M solution of potassium *tert*-butoxide (4 mmol) in anhydrous THF at room temperature. The mixture was stirred at ambient temperature for 24 h. The reaction mixture was then poured into 200 mL of methanol with stirring. The resulting green precipitate was washed with deionized water and dried under vacuum to afford 0.21 g (yield 87%) of a green powder. **P1:** <sup>1</sup>H NMR (CDCl<sub>3</sub>, ppm):  $\delta$  7.48–7.13 (br, 6H, Ar-*H* and *trans*-vinyl protons), 7.08–6.75 (br, 6H, Ar-*H*), 4.58–4.09 (br, 4H, –OCH<sub>2</sub>CH<sub>2</sub>N–), 3.68–3.44 (br, 4H, –OCH<sub>2</sub>CH<sub>2</sub>N–), 3.43–3.00 (br, 8H, –NCH<sub>2</sub>CH<sub>3</sub>), 1.59–1.18 (br, 12H, –NCH<sub>2</sub>CH<sub>3</sub>). FT-IR (KBr pellet, cm<sup>–1</sup>): 3400 (br), 3034, 2967, 2930, 2872, 2806, 1608, 1575, 1517, 1485, 1383, 1290, 1243, 1176, 1110, 1052, 1031, 975, 904, 834, 736, 656, 541. Anal. Calcd for (C<sub>32</sub>H<sub>40</sub>N<sub>2</sub>O<sub>2</sub>)<sub>n</sub>: C, 79.30; H, 8.32; N, 5.78. Found: C, 76.01; H, 7.95; N, 6.03.

**b. General Procedure for the Preparation of P2 and P3 via Wittig Reaction.** A solution of 0.476 g (7.0 mmol) of sodium ethoxide in 7 mL of anhydrous ethanol was added to a stirred solution of 1.00 g (0.87 mmol) of triphenylphosphonium chloride monomer **2** and 0.87 mmol of diformyl monomer (0.518 g of monomer **3** or 0.529 g of monomer **4**) in 10 mL of dry chloroform and 10 mL of anhydrous ethanol. The mixture was stirred for 12 h and then poured into 200 mL of methanol. The green powder was collected by filtration and further purified by a Soxhlet extraction in methanol for 3 days.

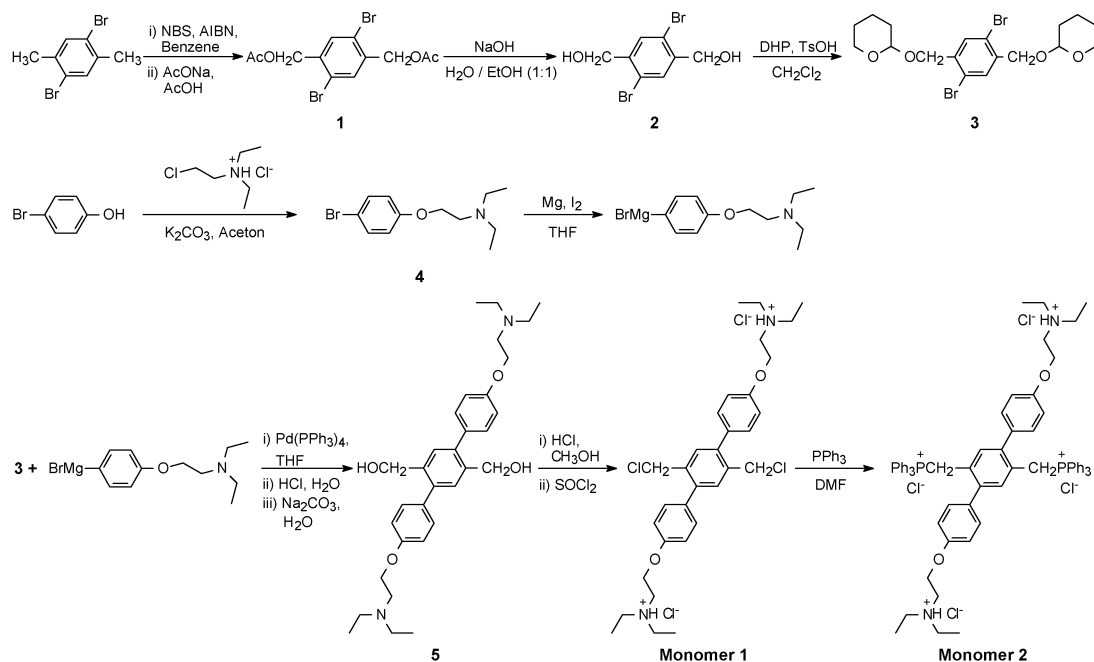
**P2:** 0.61 g (yield 67%). <sup>1</sup>H NMR (CDCl<sub>3</sub>, ppm):  $\delta$  7.73–7.46 (br, Ar-*H*), 7.46–7.24 (br, Ar-*H* and *trans*-vinyl protons), 7.24–6.97 (br, Ar-*H*), 6.97–6.87 (br, Ar-*H*), 6.87–6.65 (br, Ar-*H*), 6.59–6.36 (br, *cis*-vinyl protons), 4.20–4.06 (br, –OCH<sub>2</sub>– in *trans*-vinyl groups), 4.06–3.93 (br, –OCH<sub>2</sub>C<sub>9</sub>H<sub>19</sub>– in *cis*-vinyl protons), 3.93–3.79 (br, –OCH<sub>2</sub>– in *cis*-vinyl protons), 3.03–2.76 (m, 4H, –OCH<sub>2</sub>CH<sub>2</sub>N–), 2.76–2.52 (m, 8H, –NCH<sub>2</sub>CH<sub>3</sub>), 1.96–1.59 (br, 8H, –OCH<sub>2</sub>CH<sub>2</sub>CH<sub>2</sub>–), 1.57–1.18 (br, 24H, –(CH<sub>2</sub>)<sub>6</sub>CH<sub>3</sub>), 1.18–0.96 (m, 12H, –NCH<sub>2</sub>CH<sub>3</sub>), 0.96–0.79 (br, 6H, –(CH<sub>2</sub>)<sub>6</sub>CH<sub>3</sub>). <sup>13</sup>C NMR (CDCl<sub>3</sub>, ppm):  $\delta$  158.71, 139.35, 134.60, 133.15, 131.97, 130.90, 130.10, 114.33, 68.27, 66.79, 52.16, 48.20, 32.29, 29.97, 29.83, 29.72, 26.51, 23.02, 14.46, 12.31. FT-IR (KBr pellet, cm<sup>–1</sup>): 3406 (br), 3034, 2961, 2924, 2853, 2808, 1686, 1609, 1574, 1518, 1468, 1422, 1385, 1292, 1246, 1175, 1111, 1053, 1030, 1009, 937, 914, 875, 831, 731, 652, 540. Anal. Calcd for (C<sub>72</sub>H<sub>98</sub>N<sub>2</sub>O<sub>4</sub>)<sub>n</sub>: C, 82.24; H, 9.01; N, 2.66. Found: C, 81.50; H, 8.70; N, 2.87.

**P3:** 0.58 g (yield 63%). <sup>1</sup>H NMR (CDCl<sub>3</sub>, ppm):  $\delta$  7.68–7.46 (br, Ar-*H*), 7.43–7.22 (br, Ar-*H* and *trans*-vinyl protons), 7.22–6.99 (br, Ar-*H*), 6.99–6.88 (br, Ar-*H*), 6.88–6.65 (br, Ar-*H*), 6.58–6.33 (br, *cis*-vinyl protons), 4.28–3.44 (br, 28H, –OCH<sub>2</sub>–), 3.43–3.26 (br, 6H, –OCH<sub>3</sub>), 3.03–2.77 (m, 4H, –OCH<sub>2</sub>CH<sub>2</sub>N–), 2.77–2.50 (m, 8H, –NCH<sub>2</sub>CH<sub>3</sub>), 1.26–0.95 (m, 12H, –NCH<sub>2</sub>CH<sub>3</sub>). <sup>13</sup>C NMR (CDCl<sub>3</sub>, ppm):  $\delta$  158.44, 158.33, 139.37, 134.58, 133.25, 131.93, 130.90, 129.98, 114.45, 72.29, 71.18, 71.02, 70.91, 70.10, 67.79, 66.78, 59.34, 52.16, 48.14, 12.31. FT-IR (KBr pellet, cm<sup>–1</sup>): 3477 (br), 3032, 2964, 2926, 2875, 2820, 1686, 1608, 1573, 1520, 1471, 1422, 1379, 1353, 1293, 1246, 1203, 1178, 1111, 1064, 1032, 1009, 915, 875, 833, 808, 733, 651, 540. Anal. Calcd for (C<sub>66</sub>H<sub>82</sub>N<sub>2</sub>O<sub>10</sub>)<sub>n</sub>: C, 74.55; H, 7.77; N, 2.63. Found: C, 73.15; H, 7.39; N, 3.50.

**General Procedure for the Preparation of P2' and P3' via Postquaternization on Neutral Polymers (P2 and P3, Respectively).** A 50 mL round-bottom flask with a magnetic spin bar was charged with 0.40 mmol of neutral polymer (0.420 g for **P2** or 0.425 g for **P3**) dissolved in 20 mL of THF. To this was added bromoethane (0.436 g, 4 mmol) and 5 mL of DMSO. The solution was stirred at 50 °C for 3 days, and then most of the bromoethane and THF was evaporated. Polymer was precipitated in 100 mL of acetone, collected by centrifugation, and dried overnight in a vacuum at 50 °C.

**P2':** 0.38 g (yield 75%). <sup>1</sup>H NMR (CDCl<sub>3</sub>, ppm):  $\delta$  7.90–6.10 (br, 24H, Ar-*H* and vinyl protons), 4.71–3.00 (br, –OCH<sub>2</sub>– and –NCH<sub>2</sub>–), 2.00–0.60 (br, 54.8H, –(CH<sub>2</sub>)<sub>8</sub>CH<sub>3</sub> and –NCH<sub>2</sub>CH<sub>3</sub>). <sup>13</sup>C NMR (CDCl<sub>3</sub>, ppm):  $\delta$  159.82, 158.55,

Scheme 1. Synthetic Routes for Monomers 1 and 2



140.08, 135.93, 135.16, 133.16, 131.80 (br), 115.66, 69.24, 63.63, 62.86, 57.35, 55.15, 52.33, 33.08, 30.73, 30.44, 27.23, 23.72, 14.57, 9.35, 8.18. FT-IR (KBr pellet, cm<sup>-1</sup>): 3409 (br), 3033, 2926, 1684, 1608, 1574, 1518, 1469, 1422, 1393, 1292, 1243, 1177, 1111, 1060, 1025, 1009, 937, 915, 875, 833, 728, 652, 540. Anal. Calcd for (C<sub>72</sub>H<sub>94</sub>N<sub>2</sub>O<sub>4</sub>·1.8C<sub>2</sub>H<sub>5</sub>Br·3H<sub>2</sub>O)<sub>n</sub>: C, 69.76; H, 8.44; N, 2.15; Br, 11.05. Found: C, 67.96; H, 7.58; N, 1.93; Br, 12.59.

**P3**: 0.35 g (yield 68%). <sup>1</sup>H NMR (CDCl<sub>3</sub>, ppm): δ 7.80–6.20 (br, 24H, Ar-*H* and vinyl protons), 4.60–3.20 (br, -OCH<sub>2</sub>- and -NCH<sub>2</sub>-), 1.80–0.80 (br, 17.1H, -(CH<sub>2</sub>)<sub>8</sub>CH<sub>3</sub> and -NCH<sub>2</sub>CH<sub>3</sub>). <sup>13</sup>C NMR (CDCl<sub>3</sub>, ppm): δ 159.57, 158.49, 140.28, 135.79, 135.30, 132.91, 131.79 (br), 130.54, 115.67, 72.99, 71.77, 71.57, 71.38, 70.79, 68.65, 63.57, 62.95, 59.15, 57.30, 55.11, 52.26, 9.35, 8.14. FT-IR (KBr pellet, cm<sup>-1</sup>): 3429 (br), 3032, 2979, 2926, 2879, 2824, 1686, 1608, 1574, 1520, 1470, 1422, 1395, 1353, 1293, 1246, 1178, 1111, 1062, 1029, 1009, 941, 919, 875, 835, 786, 733, 651, 540. Anal. Calcd for (C<sub>66</sub>H<sub>82</sub>N<sub>2</sub>O<sub>10</sub>·1.7C<sub>2</sub>H<sub>5</sub>Br·5H<sub>2</sub>O)<sub>n</sub>: C, 62.27; H, 7.57; N, 2.09; Br, 10.15. Found: C, 60.38; H, 6.59; N, 1.71; Br, 11.54.

## Results and Discussion

**Synthesis of Monomers and Polymers.** The preparation of monomers was shown in Schemes 1 and 2. Compound 3 was prepared from 2,5-dibromo-*p*-xylene according to the following reaction sequences: free-radical bromination with NBS, esterification, hydrolysis, and protection of hydroxy groups with DHP. Compound 4 was prepared from 4-bromophenol by Williamson ether reaction with 2-chlorotriethylamine hydrochloride in refluxing acetone. Palladium-catalyzed aryl-aryl coupling between compounds 3 and 4 afforded compound 5 as white crystals, which was converted to the key monomer 1, 2,5-bis[4'-2-(*N,N*-diethylamino)ethoxyphenyl]-1,4-bis(chloromethyl)benzene dihydrochloride, through acid-assisted deprotection and chlorification with thionyl chloride. It is worth noting that the tertiary amine groups must be protected with chloric acid before the formation of monomer 1 to prevent the self-quaternization with benzyl chloride groups.<sup>27</sup> Monomer 2 was then obtained from monomer 1 by reaction with PPh<sub>3</sub>. Monomers 3 and 4 were prepared in a similar way from compounds 7 and 13, respectively, through consecutive

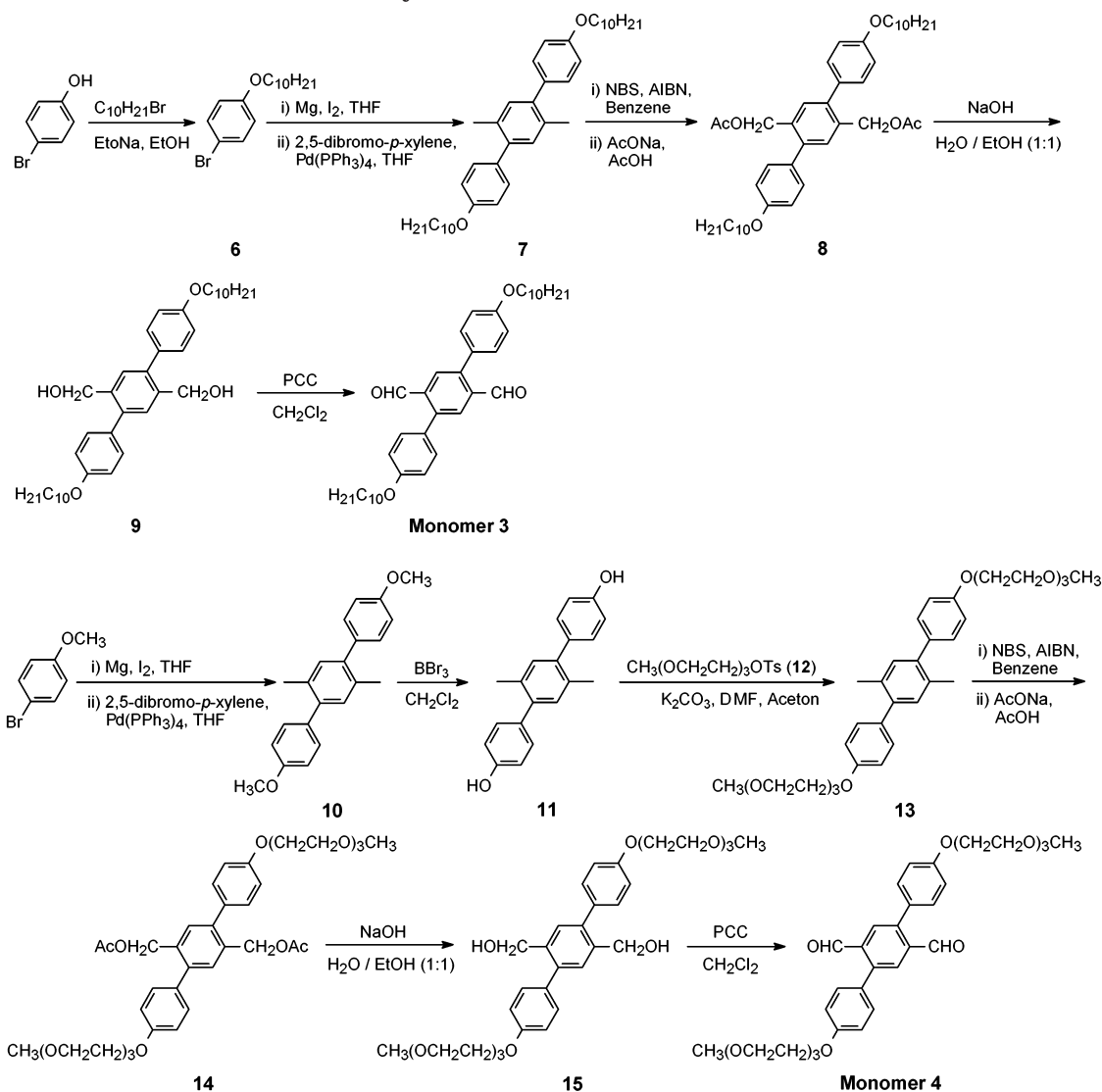
NBS bromination, esterification, hydrolysis, and PCC oxidation. Compounds 7 and 13 were both obtained via Grignard coupling reaction. However, for compound 7, a decyloxy group was introduced before the coupling reaction while the tri(ethylene glycol)methyl ether functionality was introduced for compound 13 after the coupling reaction.

Syntheses of the polymers were outlined in Scheme 3. While **P1** was obtained through Gilch reaction with *t*-BuOK in THF at room temperature, both **P2** and **P3** were synthesized via Wittig reaction between corresponding monomers in a mixture of chloroform and ethanol (1:1) containing C<sub>2</sub>H<sub>5</sub>ONa at room temperature. Conversion of the neutral polymers to the corresponding cationic polymers was achieved by stirring with bromoethane in DMSO/THF (1:4) at 50 °C for 5 days. Such a postquaternization approach has the advantage that the neutral polymers, **P2** and **P3** here, can be purified easily and characterized clearly.<sup>17b</sup>

**Solubility Studies.** With tertiary amine side chains, **P1** was quickly precipitated in the potassium *tert*-butoxide-THF system during the Gilch reaction. The obtained bright yellow powder could not be dissolved in common solvents such as THF and CHCl<sub>3</sub>, indicating that the tertiary amine side chains are not longer enough to make such rigid phenyl-substituted PPV soluble, although it appeared to be a little swelled in CHCl<sub>3</sub>. Therefore, preparation of quaternized **P1** is impossible through postpolymerization due to its insolubility. In an attempt to improve the solubility, **P2** and **P3** with longer flexible side chains were designed. To compare the effect of hydrophilicity of the side chains on water solubility of the polymers, decyloxy or tri(ethylene glycol)methyl ether groups were employed. Both **P2** and **P3** showed excellent solubility in common organic solvents such as THF and CHCl<sub>3</sub>, but they were insoluble in polar ones such as DMSO, CH<sub>3</sub>OH, and H<sub>2</sub>O. Quaternization of neutral **P2** and **P3** was thus performed in THF/DMSO (4:1) mixtures. The obtained **P2'** and **P3'** could be dissolved in DMSO, DMF, and CH<sub>3</sub>OH, indicating enhanced polarity due to quaterniza-



Scheme 2. Synthetic Routes for Monomers 3 and 4



tion. In addition, while **P2'** was completely insoluble in water, **P3'** could be successfully dissolved in warm water at 50 °C, and no precipitate was observed at room temperature even after standing still for 3 months, showing that a relatively stable aqueous solution was formed. On the basis of the above observation, it was suggested that the use of hydrophilic functionality such as tri(ethylene glycol)methyl ether groups as the side chains be crucial in obtaining intrinsically water-soluble conjugated polymers with an alternating substitution pattern.

The intractable **P1**, however, could be soluble in some polar solvents including  $\text{CHCl}_3$ ,  $\text{MeOH}$ , and water by adding organic acid (1 M) such as acetic acid. Such an interesting phenomenon of acid-assisted solubility exhibited in many solvents for amine-functionalized conjugated polymers as described in our previous work,<sup>26b</sup> which may be attributed to relatively strong intermolecular interactions between the polymer and the acid introduced. In addition, it was also found that such a polymer/acid "complex" was unstable in a vacuum. For example, when **P1** in acetic acid– $\text{CHCl}_3$  solution was precipitated in hexane and dried in a vacuum at 60 °C for 3 days, the resulting solid could not be dissolved in  $\text{CHCl}_3$  any more unless acetic acid was readded. The FT-IR spectrum of such **P1** precipitate was the same

as that of pristine **P1** in which no carboxyl absorption attributable to acetic acid appeared at about  $1680\text{ cm}^{-1}$ , indicating completely removal of the acid from the "complex". It is well-known that conjugated polymers with similar solubility are unsuitable for construction of a multilayer light-emitting diode due to the unfavorable damage of the polymer–polymer interface which may influence the quantum efficiency of the device. Therefore, the versatile acid-assisted and interesting reversible solubility for **P1** may find applications in fabricating multiplayer optoelectronic devices through a spin-coating approach.

**FT-IR Analysis.** Infrared spectra for all polymers are shown in Figure 1. As the structure difference among **P1**–**P3** only lies in the different side chains attached to the phenylene rings, IR spectra of these polymers were similar to each other. It can be seen that a weak absorption, which can be attributed to the aldehyde end groups for **P2** and **P3**, occurs at  $1680\text{ cm}^{-1}$ , indicating incomplete intermolecular condensation. Interestingly, it was also found that the ratio of *trans*- $\text{CH}=\text{CH}$  ( $\sim 975\text{ cm}^{-1}$ ) group to *cis*- $\text{CH}=\text{CH}$  ( $\sim 875\text{ cm}^{-1}$ ) group in the IR spectrum of **P1** was rather different from that of **P2** and **P3**. A weak absorption peaked at  $975\text{ cm}^{-1}$  was clearly visible for **P1** while no signals could be found at  $875\text{ cm}^{-1}$ , indicating that **P1** predominantly contains a

## Scheme 3. Synthetic Routes for the Polymers

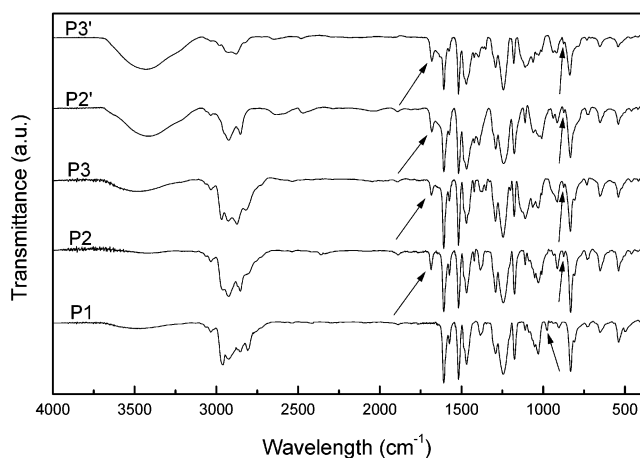
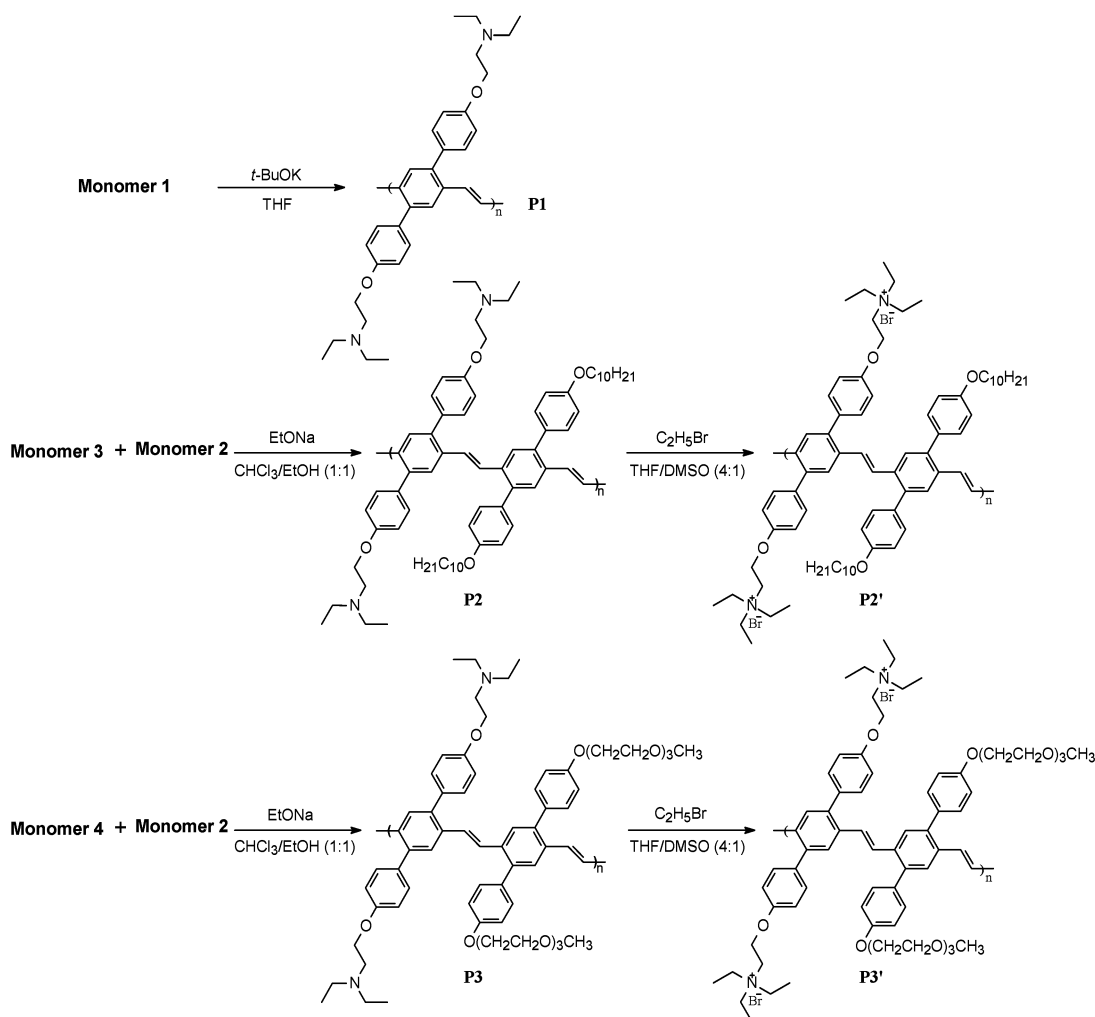


**Figure 1.** FT-IR spectra of the neutral and quaternized Ph-PPVs.

*trans*-CH=CH group under Gilch conditions. On the contrary, a high ratio of *cis*-CH=CH group to *trans*-CH=CH was observed on the basis of the IR measurements for **P2** and **P3** which were obtained through Wittig reaction. Therefore, it is concluded that Gilch reaction is more suitable for developing polymers with regular molecular configurations than Wittig reaction. However, the ratio of *trans*- vs *cis*-configuration cannot be determined by the FT-IR spectrum, which will be discussed in the next section.

Upon quaternization, all the quaternized polymers showed some spectral modifications due to new substituents formed while the spectral features of the intact structures in the polymers remained unchanged in the FT-IR spectra. Besides, a broad and strong self-associated absorption peak of water at  $3400\text{ cm}^{-1}$  can be observed, which reflects strong hydrophilicity of the resulting quaternized polymers.

**NMR Analysis.**  $^1\text{H}$  NMR spectra of all the neutral and quaternized polymers are shown in Figure 2. Integration ratios of the end aldehyde protons (10.01 ppm) to the  $-\text{OCH}_2\text{CH}_2\text{N}-$  protons for **P2** and **P3** (3.00–2.76 ppm) were found to be about 1/30 and 1/32, respectively, corresponding to 15 and 16 phenyl rings in the backbone, respectively. These results are in good agreement with those measured by GPC (Table 1). Our FT-IR analysis showed that **P1** adopted predominantly the *trans*-CH=CH configuration while for **P2** and **P3**, a high content of *cis*-CH=CH groups was present. Such a result was also substantiated by  $^1\text{H}$  NMR measurements. The  $^1\text{H}$  NMR spectrum of **P1** was rather simple compared with **P2** and **P3**, indicating a more regular structure for **P1**. On the basis of the spectral simplicity for **P1** as well as the structural similarity among **P1**, **P2**, and **P3**, it is easy to realize that there were two groups of resonances for the protons of **P2** and **P3**, in which the downfield and upfield ones caused by the *trans*- and *cis*-configurations, respectively.<sup>28</sup> Although the *cis*- and *trans*-vinyl protons can be observed at 6.50

Table 1. GPC and Spectroscopic Data for Ph-PPVs

polymer	GPC			absorbance		fluorescence <sup>g</sup>			
	$M_n^a$	$M_w^a$	PDI <sup>a</sup>	in solution	film	in solution		film	
				$\lambda_{\max}$ (nm)	$\lambda_{\max}$ (nm)	$\lambda_{\max}$ (nm)	$\Phi_{\text{pl}}$	$\lambda_{\max}$ (nm)	$\Phi_{\text{pl}}$
<b>P1</b>				416 <sup>b</sup>	420	494 <sup>b</sup>	0.52	505	0.51
<b>P1</b>				412 <sup>c</sup>		483 <sup>c</sup>	0.18		
<b>P2</b>	8600	12 000	1.40	387 <sup>d</sup>	387	495 <sup>d</sup>	0.51	507	0.58
<b>P3</b>	8200	10 600	1.29	387 <sup>d</sup>	389	493 <sup>d</sup>	0.51	505	0.56
<b>P2'</b>				370 <sup>e</sup>	380	483 <sup>e</sup>	0.28	496	0.17
<b>P3'</b>				377 <sup>e</sup>	380	483 <sup>e</sup>	0.25	495	0.13
<b>P3'</b>				368 <sup>f</sup>		481 <sup>f</sup>	0.15		

<sup>a</sup>  $M_n$ ,  $M_w$ , and PDI of the polymers were determined by gel permeation chromatography using polystyrene standards. <sup>b</sup> The values listed were measured in acetic acid-CHCl<sub>3</sub> solution (1 M). <sup>c</sup> In acetic acid-H<sub>2</sub>O solution (1 M). <sup>d</sup> In THF. <sup>e</sup> In methanol. <sup>f</sup> In water. <sup>g</sup> The  $\Phi_f$  values of those polymers in solutions were measured using the quinine sulfate solution (ca.  $1.0 \times 10^{-5}$  M) in 0.10 M H<sub>2</sub>SO<sub>4</sub> ( $\Phi_f = 55\%$ ) as a standard. The  $\Phi_f$  values of those polymers as films were measured using diphenylanthracene (dispersed in PMMA film with a concentration less than  $10^{-3}$  M, assuming  $\Phi_f = 81\%$ ) as a standard.

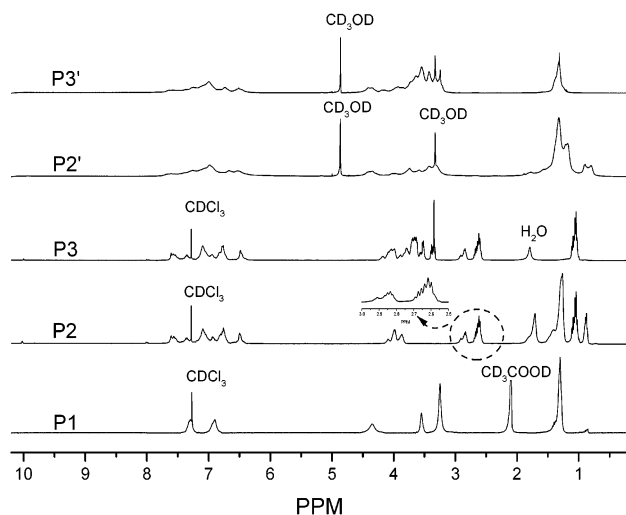


Figure 2. <sup>1</sup>H NMR spectra of the neutral and quaternized Ph-PPVs.

and 7.36 ppm, respectively, with the former to be much more intensive, the ratios of *cis*- to *trans*-vinyl groups were determined by comparing the relative integrations of the *cis*-CH=CH resonance at 6.50 ppm with the -OCH<sub>2</sub>CH<sub>2</sub>N- resonance between 3.00 and 2.78 ppm. As a result, the contents of *cis*-configurations for **P2** and **P3** were calculated to be 80% and 81%, respectively. It is well-known that in normal Wittig reactions both *trans*- and *cis*-vinyl are formed. Such high values of *cis*-configuration in the present work may be related to the steric effect due to bulky phenylene substituents which may also affect the main chain conformations of such PPV-type polymers.

Quaternization with bromoethane led to broadened proton peaks, some of which could not be identified. It can be seen in Figure 2, however, that the aromatic protons of the quaternized polymers resonance at the same chemical shifts compared with those of the corresponding neutral ones, whereas **P2'** and **P3'** exhibit spectra in which all the signals from -OCH<sub>2</sub>CH<sub>2</sub>N-, -NCH<sub>2</sub>CH<sub>3</sub>, and -NCH<sub>2</sub>CH<sub>3</sub> groups are downshifted. The quaternization degrees (QD) could be determined from the <sup>1</sup>H NMR spectra by comparing the relative integrations of the aromatic peaks at 6.0–8.0 ppm (total aromatic and vinyl protons) with that of 0.5–2.0 ppm (total alkyl protons for -OCH<sub>2</sub>C<sub>9</sub>H<sub>19</sub> and -NCH<sub>2</sub>CH<sub>3</sub> in **P2'** or -NCH<sub>2</sub>CH<sub>3</sub> in **P3'**).<sup>29</sup> As a result, the QDs of **P2'** and **P3'** were calculated to be about 90% and 85%, respectively, which were close to the results from elemental analysis.

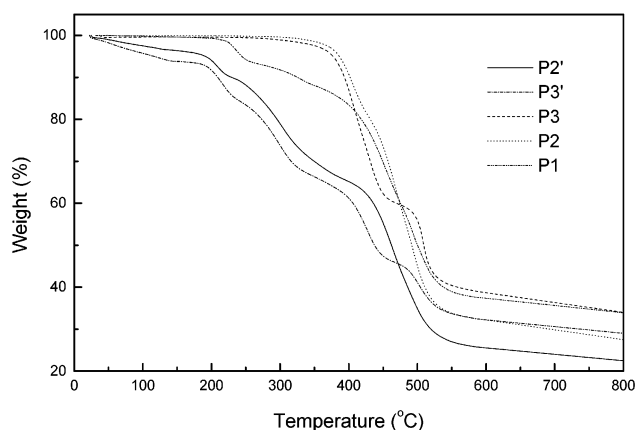
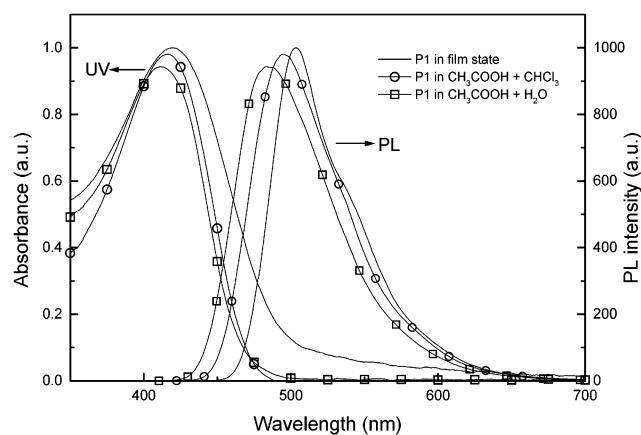


Figure 3. Thermogravimetric analysis of the neutral and quaternized Ph-PPVs.

**Thermal Stability.** Thermal properties of the polymers were studied by thermogravimetric analysis (TGA) under a nitrogen atmosphere. The thermograms in Figure 3 showed that the neutral polymers **P2** and **P3** exhibited good thermal stability with a weight loss of 3% at 340 °C. However, **P1** gave an initial degradation at 220 °C, which is considerably lower than those of **P2** and **P3**. Such a decrease of thermostability for **P1** may be attributed to the molecular impurities encapsulated by **P1** when it was precipitated from the reaction mixture. For the quaternized samples, the degradation onsets for **P2'** and **P3'** decreased to 200 °C with the initial weight loss deriving from associated water. This variation can be explained by the lower stability of ethyl bromide than that of the other alkoxy side chains.<sup>17b</sup> The relatively high thermostability thus renders these polymers good candidates in light-emitting diodes and fluorescent sensor uses.

**Optical Properties.** The optical properties of **P1** were investigated, and the absorption and emission spectra in CHCl<sub>3</sub> or H<sub>2</sub>O containing acetic acid (1 M) and as film are shown in Figure 4. It was found that both absorption and emission spectra in CHCl<sub>3</sub> are more red-shifted than those in H<sub>2</sub>O. Although the spectral changes in different solvents may result from the solvatochromism due to the polarity of the solvents, the bathochromic shift in CHCl<sub>3</sub> is unlikely caused by the stabilization of the ground state as well as the excited state by the solvent based on the fact that CHCl<sub>3</sub> is less polar than water, which would lead to a hypochromic shift in the spectra. It should be more reasonable to consider the different molecular conformation of the polymer in different solvents. It has been reported that



**Figure 4.** UV-vis absorption and PL emission spectra of **P1** in acetic acid- $\text{CHCl}_3$  solution (1 M) and in acetic acid aqueous solution (1 M) and as films.

the conformation of MEH-PPV varies from extended to coiled ones depending on the quality of the solvents.<sup>30,31</sup> Accordingly, we performed a  $^1\text{H}$  NMR experiment for **P1** in  $\text{CDCl}_3$  and  $\text{D}_2\text{O}$ , both of which contained a small amount of acetic acid- $d_4$ . While the proton signals obtained in  $\text{CDCl}_3$  are clearly distinguishable, those in  $\text{D}_2\text{O}$  cannot be observed even when the number of scans was 10 000. It is generally accepted that decrease of solvent quality causes a corresponding reduction of magnetic resonance signature. Therefore, we believe that  $\text{H}_2\text{O}$  is a poor solvent, and **P1** tends to be less solvated. The hypochromic shift of **P1** found in  $\text{H}_2\text{O}$  is consistent with the reduced solvent quality, indicating a coiled molecular conformation which causes a shorter average conjugation length.<sup>30,31</sup> In addition, fluorescence quantum efficiencies ( $\Phi_f$ ) were also measured, and the findings showed that **P1** gave a lower  $\Phi_f$  of 18% in  $\text{H}_2\text{O}$  than that in  $\text{CHCl}_3$  (52%). To examine the possible contribution of aggregation effects to such a decrease, the absorption and emission spectra of **P1** as film (spin-cast from  $\text{CHCl}_3$  solution) were studied, both of which (420 and 505 nm, respectively) presented slightly red-shifted spectral maxima as compared with those in solutions. There is no evidence showing the formation of interchain dimers or excimers.  $\Phi_f$  of this film (51%) was found to be comparable with that in solution (52%). On the basis of the above observations, intermolecular aggregation should play a less important role in the lower fluorescence yield of **P1** in water, although it may exist. Therefore, such a decrease in  $\Phi_f$  may also be explained by the coiled molecular structure of the polymer backbone which contains a lot of torsional defects.<sup>30</sup>

The UV-vis absorption and photoluminescence (PL) spectra of the neutral and quaternized polymers **P2**, **P3**, **P2'**, and **P3'** in solution are depicted in Figure 5. The same absorption maxima at 387 nm and emission maxima at 494 nm exhibited by both **P2** and **P3** imply that the electronic properties of these phenyl-substituted polymers are predominantly determined by the rigid PPV main chain while those flexible chains play a minor role. The absorption maxima of the neutral polymers **P2** and **P3** in solution blue-shifted considerably as compared with that of *trans*-type poly{2-(4'-decyloxyphenyl)-1,4-phenylenevinylene (DOP-PPV) (410 nm),<sup>32</sup> which is in agreement with the high content of *cis*-vinyl bonds in **P2** and **P3** with reduced effective conjugation length.

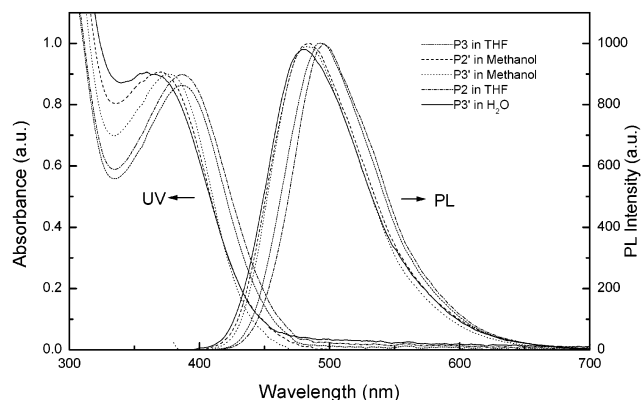


**Figure 5.** UV-vis absorption and PL emission spectra of **P2** and **P3** in THF, **P2'** and **P3'** in methanol, and **P3'** in water.

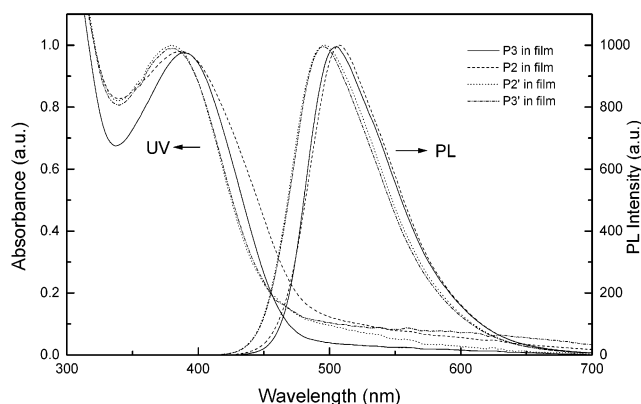


**Figure 6.** UV-vis absorption and PL emission spectra of **P2**, **P3**, **P2'**, and **P3'** as films.

Quaternization was found to create more obvious blue-shifted absorption and fluorescence spectra and result in decreased  $\Phi_f$  for **P2'** and **P3'**, as shown in Figure 5 and Table 1. Such a blue shift, attributable to the mutual electrostatic repulsion of positive charges pendent on the alternating benzene rings which leads to an increased torsion of the conjugated main chain and a decreased effective conjugation length,<sup>17b,26b</sup> was observed in other quaternized systems. We also found that quaternization resulted in reduced  $\Phi_f$  of **P2'** and **P3'** which may be caused by the torsion induced quenching as the planarization in the excited state is impeded.<sup>33</sup>  $^1\text{H}$  NMR measurement showed that water is a poorer solvent for **P3'** than methanol. As a result, the blue-shifted electronic spectra and decreased  $\Phi_f$  exhibited by **P3'** in water as compared with those measured in methanol suggested the more coiled structure adopted in water as we discussed for **P1**. We will demonstrate later that intermolecular aggregation may not contribute so much to such a decrease.

When the absorption and emission spectra of these polymers as films were investigated, blue-shifted spectral maxima as shown in Figure 6 were observed for quaternized polymers as compared with their respective precursors. This indicates that the modified conformation of the quaternized polymers in solution was maintained in their respective films. In addition, almost the same spectral features and  $\Phi_f$  exhibited by the neutral polymers in both solution and the solid state suggest that the formation of interchain dimers and excimers is negligible due to the steric effect of the two phenyl rings and the strong intermolecular electrostatic repulsion as films. Therefore, although intermolecular aggregation



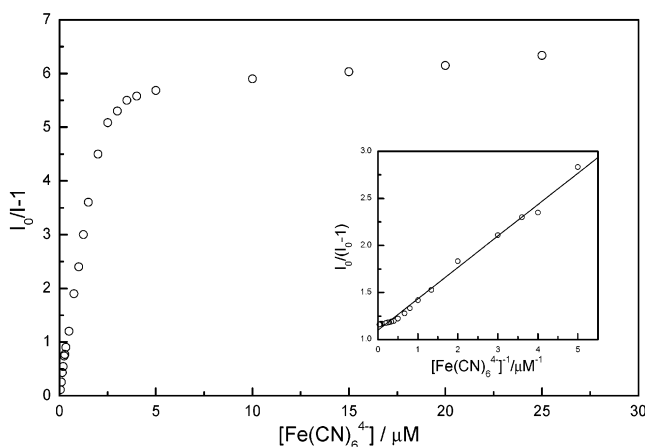


**Figure 7.** Unmodified Stern–Volmer plot of **P3'** (1.25  $\mu\text{M}$ ) quenched by  $\text{Fe}(\text{CN})_6^{4-}$ . Inset: modified Stern–Volmer plot of **P3'**.

(association) was observed with a few WSCPs in water,<sup>34</sup> such interchain interactions do not cause significant decrease in fluorescence yield in our systems.

**Fluorescent Quenching of P3'.** One promising application of WSCPs is for chemo- or biosensors due to their fluorescent superquenching by traces of analytes. The quenching of fluorescence generally includes static quenching and dynamic quenching. Each quenching behavior can be simply described by the Stern–Volmer equation:<sup>35</sup>

$$F_0/F = 1 + K_{\text{sv}}[Q] \quad (1)$$

In this equation,  $F_0$  is the fluorescence intensity with no quencher present,  $F$  is the fluorescence intensity with quencher present,  $[Q]$  is the quencher concentration, and  $K_{\text{sv}}$  is the Stern–Volmer constant. Both dynamic and static quenching follow a linear Stern–Volmer plot ( $F_0/F \sim [Q]$ ). However, if the dynamic quenching and static quenching exist simultaneously, eq 1 must be modified, and the plot shows an upward curve:<sup>35</sup>

$$F_0/F = (1 + K_{\text{sv}}^{\text{S}}[Q])(1 + K_{\text{sv}}^{\text{D}}[Q]) \quad (2)$$

where  $K_{\text{sv}}^{\text{S}}$  is the static quenching constant and  $K_{\text{sv}}^{\text{D}}$  is the dynamic quenching constant. Previously, both the linear and upward Stern–Volmer curves were observed with WSCPs.<sup>20,21c,d,22</sup>

As a cationic WCPs, **P3'** was employed to detect anionic analyte,  $\text{Fe}(\text{CN})_6^{4-}$ , to study its sensing behavior.  $\text{Fe}(\text{CN})_6^{4-}$  has been used to investigate a cationic PPP polymer<sup>22</sup> as a quencher, of which both the energy transfer and photoinduced electron-transfer processes may be involved in the quenching mechanism, depending on the type of the chromophores. Figure 7 shows the Stern–Volmer plot for **P3'** with  $\text{Fe}(\text{CN})_6^{4-}$  as the quencher. It can be seen that an intriguing downward Stern–Volmer curve was observed, which has never been reported with fluorescent WSCPs. Therefore, it is reasonable to believe that some other influencing factors may work.

Such a downward Stern–Volmer plot was observed during the study of fluorescent quenching of tryptophan in proteins using iodide and explained by the existence of two populations of fluorophores, one of which is inaccessible to the quencher.<sup>36</sup> Therefore, with the introduction of a quencher, only those accessible fluorophores are quenched while the fluorescence from the

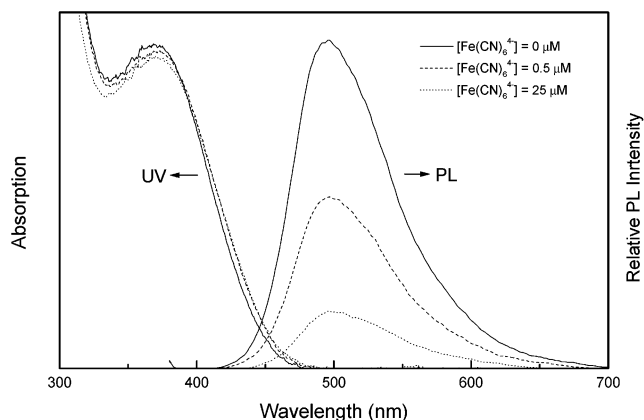


**Figure 8.** UV–vis absorption and PL emission spectra of **P3'** (1.25  $\mu\text{M}$ ) in the absence and presence of  $\text{Fe}(\text{CN})_6^{4-}$ .

inaccessible ones remains. On the basis of the above assumption, a quantitative expression was given to describe the relation between the fluorescence intensity and quencher concentration:<sup>37</sup>

$$F_0/(F_0 - F) = 1/(f_a K_{\text{sv}}[Q]) + 1/f_a \quad (3a)$$

$$f_a = F_{0a}/(F_{0a} + F_{0b}) \quad (3b)$$

where  $F_{0a}$  is the fluorescence intensity from an accessible fluorophore,  $F_{0b}$  is the fluorescence intensity from an inaccessible fluorophore, and  $f_a$  is the fraction of fluorescence from an accessible fluorophore. The modified Stern–Volmer plot for **P3'** according to eq 3a was shown in the inset of Figure 7, and a linear dependence of  $F_0/(F_0 - F)$  on  $1/[\text{Fe}(\text{CN})_6^{4-}]$  can be observed. On the basis of the intercept and the slope,  $f_a = 0.91$  and  $K_{\text{sv}} = 3.3 \times 10^6 \text{ M}^{-1}$  were obtained. Such a value of  $K_{\text{sv}}$  did indicate an efficient fluorescence quenching of **P3'**, which was bound with the quencher through static electronic interaction. Approximately 7–8 phenyl rings in the polymer backbone per quencher can also be estimated, which corresponds to almost one polymer chain per two quenchers.<sup>38</sup> 9% of the inaccessible fluorophores might result from the proposed twisted and coiled backbone conformation and possible intermolecular aggregation due to poor solvent quality.

It is important to note that additions of multivalent cations may tend to increase the aggregation resulting in interchain quenching.<sup>20,21d</sup> However, as discussed earlier, such an additional aggregation does not significantly affect the quantum efficiency of **P3'** due to the bulky phenylene substituents. In addition, both absorption and emission spectra for **P3'** obtained with the addition of  $\text{Fe}(\text{CN})_6^{4-}$  exhibited minor spectral changes in terms of the shape and wavelength of the peaks, as shown in Figure 8,<sup>39</sup> indicating that intermolecular ground-state and excited-state complex were absent. It is also suggested that quencher-induced aggregation may be minimal, considering the relatively low concentration of **P3'** in the mixture (as low as 1.25  $\mu\text{M}$ ).<sup>20</sup> Therefore, it is fluorophore–quencher interaction (electron or energy transfer) that was involved in the quenching of **P3'**.

## Conclusions

In this work we have shown that, by means of suitable functional modifications, a series of novel water-soluble cationic green light-emitting polymers can be success-



fully synthesized through a postpolymerization approach. Two traditional polymerization techniques, Gilch and Wittig reactions, were employed and found to produce two types of polymers structures, in which *trans*- or *cis*-vinyl was the dominant composition, respectively. Although the Gilch product **P1** was insoluble in common organic solvents, its interesting acid-assisted and reversible solubility make it very promising for application as green emissive material in light-emitting diodes. Increase of hydrophilicity of the side chains was found to be beneficial to water solubility of the polymers. The optical properties of **P1** were studied, which showed a solvent-dependent conjugation length. Quaterization also resulted in the more twisted conformation of the polymer main chain. The conformation change may be responsible for the decrease in quantum efficiency of the polymers in solution. The bulky phenyl rings successfully suppressed interchain interactions, as evidenced by the absence of intermolecular dimer and excimer. Quenching studies showed that efficient fluorescence quenching can be achieved by using an anionic quencher  $\text{Fe}(\text{CN})_6^{4-}$ , which is very useful in chemo- and biosensor applications. However, a modified Stern–Volmer plot demonstrated that some of the fluophores cannot be accessible to the quencher, probably due to a twisted conformation or intermolecular aggregation.

**Acknowledgment.** This work was financially supported by Shanghai Commission of Science and Technology under Grants 022261042 and 0216nm040. Qu-Li Fan thanks the National University of Singapore and the Institute of Materials Research and Engineering (IMRE) for a research scholarship and top-up award.

**Supporting Information Available:** Experimental details and characterization of compounds **1–15** and monomers **1–4**. This material is available free of charge via the Internet at <http://pubs.acs.org>.

## References and Notes

- (1) Cimrova, V.; Schmidt, W.; Rulkens, R.; Schulze, M.; Meyer, W.; Neher, D. *Adv. Mater.* **1996**, *8*, 585.
- (2) Baur, J. W.; Kim, S.; Balanda, P. B.; Reynolds, J. R.; Rubner, M. F. *Adv. Mater.* **1998**, *10*, 1452.
- (3) Ho, P. K. H.; Granstrom, M.; Friend, R. H.; Greenham, N. C. *Adv. Mater.* **1998**, *10*, 769.
- (4) McQuade, D. T.; Pullen, A. E.; Swager, T. M. *Chem. Rev.* **2000**, *100*, 2537.
- (5) Chen, L.; Yu, S.; Kagami, Y.; Gong, J.; Osada, Y. *Macromolecules* **1998**, *31*, 787.
- (6) Decher, G. *Science* **1997**, *277*, 1232.
- (7) McCullough, R. D.; Ewbank, P. C.; Loewe, R. S. *J. Am. Chem. Soc.* **1997**, *119*, 633.
- (8) (a) Thünnemann, A. F. *Adv. Mater.* **1999**, *11*, 127. (b) Thünnemann, A. F.; Ruppelt, D. *Langmuir* **2001**, *17*, 5098.
- (9) (a) Ferreira, M.; Rubner, M. F. *Macromolecules* **1995**, *28*, 7107. (b) Fou, A. C.; Rubner, M. F. *Macromolecules* **1995**, *28*, 7115. (c) Fou, A. C.; Onitsuka, O.; Ferreira, M.; Rubner, M. F. *J. Appl. Phys.* **1996**, *79*, 7501.
- (10) Bharathan, J.; Yang, Y. *Appl. Phys. Lett.* **1998**, *72*, 2660.
- (11) Bao, Z.; Feng, Y.; Dodabalapur, A.; Raju, V. R.; Lovinger, A. J. *Chem. Mater.* **1997**, *9*, 1299.
- (12) Chang, S. C.; Bharathan, J.; Yang, Y. *Appl. Phys. Lett.* **1998**, *73*, 2561.
- (13) Baur, J. W.; Rubner, M. F.; Reynolds, J. R.; Kim, S. *Langmuir* **1999**, *15*, 6460.
- (14) Landfester, K.; Montenegro, R.; Scherf, U.; Güntner, R.; Asawapirom, U.; Patil, S.; Neher, D.; Kietzke, T. *Adv. Mater.* **2002**, *14*, 651.
- (15) Brodowski, G.; Horvath, A.; Ballauf, M.; Rehahn, M. *Macromolecules* **1996**, *29*, 6962.
- (16) Rulkens, R.; Schulze, M.; Wegner, G. *Macromol. Rapid Commun.* **1994**, *15*, 669.
- (17) (a) Kim, S.; Jackiw, J.; Robinson, E.; Schanze, K. S.; Reynolds, J. R. *Macromolecules* **1998**, *31*, 964. (b) Balanda, P. B.; Ramey, M. B.; Reynolds, J. R. *Macromolecules* **1999**, *32*, 3970.
- (18) Shi, S.; Wudl, F. *Macromolecules* **1990**, *23*, 2119.
- (19) Wagaman, M. W.; Grubbs, R. H. *Macromolecules* **1997**, *30*, 3978.
- (20) Chen, L.; McBranch, D. W.; Wang, H.-L.; Helgeson, R.; Wudl, F.; Whitten, D. G. *Proc. Natl. Acad. Sci. U.S.A.* **1999**, *96*, 12287.
- (21) (a) Chen, L.; Xu, S.; McBranch, D.; Whitten, D. G. *J. Am. Chem. Soc.* **2000**, *122*, 9302. (b) Chen, L.; McBranch, D.; Wang, R.; Whitten, D. G. *Chem. Phys. Lett.* **2000**, *330*, 27. (c) Wang, J.; Wang, D. L.; Miller, E. K.; Moses, D.; Bazan, G. C.; Heeger, A. J. *Macromolecules* **2000**, *33*, 5153. (d) Wang, D. L.; Wang, J.; Moses, D.; Bazan, G. C.; Heeger, A. J. *Langmuir* **2001**, *17*, 1262. (e) Gaylord, B. S.; Wang, S.; Heeger, A. J.; Bazan, G. C. *J. Am. Chem. Soc.* **2001**, *123*, 6417. (f) Jones, R. M.; Bergstedt, T. S.; McBranch, D. W.; Whitten, D. G. *J. Am. Chem. Soc.* **2001**, *123*, 6726. (g) Stork, M.; Gaylord, B. S.; Heeger, A. J.; Bazan, G. C. *Adv. Mater.* **2002**, *14*, 361. (h) Wang, D.; Gong, X.; Heeger, P. S.; Rininsland, F.; Bazan, G. C.; Heeger, A. J. *Proc. Natl. Acad. Sci. U.S.A.* **2002**, *99*, 49. (i) Fan, C.; Plaxco, K. W.; Heeger, A. J. *J. Am. Chem. Soc.* **2002**, *124*, 5642.
- (22) Harrison, B. S.; Ramey, M. B.; Reynolds, J. R.; Schanze, K. S. *J. Am. Chem. Soc.* **2000**, *122*, 8561.
- (23) Spreitzer, H.; Becker, H.; Kluge, E.; Kreuder, W.; Schenk, H.; Demandt, R.; Schöo, H. *Adv. Mater.* **1998**, *10*, 1340.
- (24) (a) Wan, W. C.; Antoniadis, H.; Choong, V. E.; Razafitrimo, H.; Gao, Y.; Feld, W. A.; Hsieh, B. R. *Macromolecules* **1997**, *30*, 6567. (b) Hsieh, B. R.; Yu, Y.; Forsythe, E. W.; Schaaf, G. M.; Feld, W. A. *J. Am. Chem. Soc.* **1998**, *120*, 231.
- (25) Peng, Z.; Zhang, J.; Xu, B. *Macromolecules* **1999**, *32*, 5162.
- (26) (a) Liu, B.; Yu, W.; Lai, Y. H.; Huang, W. *Chem. Commun.* **2000**, 551. (b) Liu, B.; Yu, W.; Lai, Y. H.; Huang, W. *Macromolecules* **2002**, *35*, 4975.
- (27) Stenger-Smith, J. D.; Zarras, P.; Merwin, L. H.; Shaheen, S. E.; Kippelen, B.; Peyghambarian, N. *Macromolecules* **1998**, *31*, 7566.
- (28) (a) Liao, L.; Pang, Y.; Ding, L.; Karasz, F. E. *Macromolecules* **2001**, *34*, 7300. (b) Liao, L.; Pang, Y.; Ding, L.; Karasz, F. E. *Macromolecules* **2001**, *34*, 7300.
- (29) The QDs of **P2'** and **P3'** were calculated according to the following equations:  $(50 + 6x)/24 = I_{0.5-2.0}/I_{6.0-8.0}$  and  $(12 + 6x)/24 = I_{0.5-2.0}/I_{6.0-8.0}$ , respectively, where  $x$  is the QD,  $I_{0.5-2.0}$  is the integration of the peaks at 0.5–2.0 ppm, and  $I_{6.0-8.0}$  is the integration of the peaks at 6.0–8.0 ppm.
- (30) Nguyen, T.-Q.; Doan, V.; Schwartz, B. J. *J. Chem. Phys.* **1999**, *110*, 4070.
- (31) Nguyen, T.-Q.; Schwartz, B. J. *J. Chem. Phys.* **2002**, *116*, 8198.
- (32) Pei, J.; Yu, W.-L.; Huang, W.; Heeger, A. J. *Chem. Lett.* **1999**, *10*, 1123.
- (33) Oelkrug, D.; Tompert, A.; Gierschner, J.; Egelhaaf, H.-J.; Hanack, M.; Hohloch, M.; Steinhuber, E. *J. Phys. Chem. B* **1998**, *102*, 1902.
- (34) Wang, D.; Lai, J.; Moses, D.; Bazan, G. C.; Heeger, A. J. *Chem. Phys. Lett.* **2001**, *348*, 411.
- (35) Lakowicz, J. R. In *Principles of Fluorescence Spectroscopy*, 2nd ed.; Plenum Press: New York, 1999.
- (36) Lehrer, S. S. *Biochemistry* **1971**, *10*, 3254.
- (37) Gong, Y.-K.; Miyamoto, T.; Nakashima, K.; Hashimoto, S. *J. Phys. Chem. B* **2000**, *104*, 5772.
- (38) The modified Stern–Volmer plot of **P3'** (1.25  $\mu\text{M}$ ) quenched by  $\text{Fe}(\text{CN})_6^{4-}$  showed that 50% quenching was achieved at  $[\text{Fe}(\text{CN})_6^{4-}] \approx 0.36 \mu\text{M}$ , which corresponds to approximately 7–8 phenyl rings in the polymer backbone per quencher.
- (39) The UV absorption of 10  $\mu\text{M}$   $\text{Fe}(\text{CN})_6^{4-}$  in aqueous solution was very weak and can be negligible as compared with that of 2.5  $\mu\text{M}$  **P3'** in water used in the quenching study.

MA030093F